ACS OMEGA

http://pubs.acs.org/journal/acsodf

Article

Competition and Neutralization: Thermally Induced Crystallization and Phase Evolution of Amorphous Calcium Phosphate with Cosubstitution of Larger and Smaller Divalent Cations

Lu Wang, Junxing Yang, Jianqiang Bi,* Kangning Sun, Aimin Li, and Junjie Mao

Cite This: *ACS Omega* 2023, 8, 7602−7606

Read Online

ACCESS | Metrics & More | Article Recommendations | Supporting Information

ABSTRACT: The presented study evaluated the effect of cosubstitution of larger and smaller divalent cations on the thermally induced crystallization of amorphous calcium phosphate (ACP). The predesigned combinations of larger (Sr^{2+} and Ba^{2+}) and smaller (Mg^{2+}, Cu^{2+}, and Co^{2+}) divalent cations were carried out and their effects on the thermodynamic equilibrium between α/β-tricalcium phosphate (TCP) were outlined. The coexistence of larger and smaller divalent cations shielded the formation of α-TCP and shifted the thermodynamic equilibrium toward the β-TCP, which implied that the smaller cations dominated the crystalline phase. However, the retarded crystallization induced by the larger cations still remained and allowed ACP to maintain its amorphous nature partly or completely until a higher temperature.

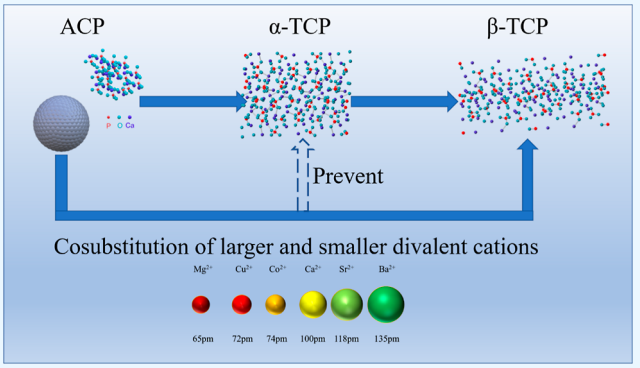

1. INTRODUCTION

Compared with crystalline phases, amorphous calcium phosphates (ACPs) draw great attention from researchers due to their unique characteristics.[1−5] Among its wide range (1.2−2.2) of Ca/P, the specific ACP under 1.5 have been widely studied for its thermally crystalline analogue is tricalcium phosphate (TCP), a universally utilized biomaterial. Benefiting from the short-range ordered structure, ACPs could transform into their crystalline analogue under appropriate thermal treatment and α-TCP was believed to be the first crystalline phase despite the fact that α-TCP was the high-temperature phase corresponding to β-TCP. Such a phenomenon was explained by the Ostwald step rule, which allowed the thermodynamically less stable phase to form primarily.[6] Compared with the traditional manufacture protocol, such a phenomenon allowed the sufficient preparation of α/β-TCP under lower temperature (600−800 °C vs 1200 °C), which served as a promising candidate. However, the amorphous nature implied that these results could be easily manipulated with the presence of foreign cations and an organic molecule. Previous study confirmed that the polyethylene glycol during the preparation process possessed a dose-dependent effect on the thermally induced crystallization and phase evolution of ACP.[7] Our previous study also proved that the introduction of inositol would postpone the crystallization of ACP and altered the thermodynamic equilibrium between α/β-TCP under higher temperature in a content-dependent manner.[8] Element substitution provided a feasible path for the multifunctionalization of traditional biomaterials and related research studies were widely carried out. The perspective research based on the theoretical calculations also proved the thermodynamic stability of substitutional divalent cations in TCP.[9] Research studies focusing on the thermally induced crystallization and phase evolution of ACP substituted by a single foreign ion have been published.[10−12] The presence of Fe^{3+} with the doping level as low as 0.1% would be sufficient enough to prevent the formation of α-TCP and obtain calcium deficient hydroxyapatite (CDHA).[13] Regarding doping with divalent cations, the larger divalent cations promoted the formation of α-TCP and even completely blocked its transition to the low temperature phase, while the smaller divalent cations promoted the formation of β-TCP.[14−18] However, there is no systematic study on the effect of the simultaneous substitution of larger and smaller ions on the thermal crystallization and phase transition of ACP. Such a research would be helpful to realize the design and preparation of multifunctional TCP.

In the present work, we selected large cations (Sr^{2+} and Ba^{2+}) and smaller cations (Mg^{2+}, Cu^{2+}, and Co^{2+}) as candidates and reported a comprehensive study on the thermally induced crystallization of ACP substituted by larger

Received: November 4, 2022
Accepted: January 23, 2023
Published: February 15, 2023

https://doi.org/10.1021/acsomega.2c07117
ACS Omega 2023, 8, 7602−7606

and smaller ions simultaneously. The thermodynamic equilibrium between α/β-TCP at low temperature (600−700 °C) was focused. The thermal properties of ACP were further investigated to explore the exothermal crystalline effect. Finally, the empirical models of the effect of cosubstitution of larger and smaller divalent ions on thermally induced crystallization of ACP were provided.

2. MATERIALS AND METHODS

2.1. Chemicals and Reagents. ACPs with cosubstitution of larger and smaller divalent cations were prepared by the wet co-precipitation method. Reagents including diammonium hydrogen phosphate [$(NH_4)_2HPO_4$, >99.0%], calcium nitrate tetrahydrate [$Ca(NO_3)_2{\cdot}4H_2O$, >99.0%], strontium chloride hexahydrate ($SrCl_2{\cdot}6H_2O$, >95.0%), magnesium chloride hexahydrate ($MgCl_2{\cdot}6H_2O$, >98.0%), copper nitrate trihydrate [$Cu(NO_3)_2{\cdot}3H_2O$, >99.0%], barium nitrate [$Ba(NO_3)_2$, >99.0%], cobalt nitrate hexahydrate [$Co(NO_3)_2{\cdot}6H_2O$, >98.5%], inositol ($C_6H_{12}O_6$, >98.0%), and ammonium hydroxide (NH_4OH, 25.0−28.0%) were acquired from Sinopharm Chemical Reagent Co., Ltd. and used as obtained without further refinement.

2.2. Material Preparation. The nominal composition of [$Ca_{2.7}L_{0.15}S_{0.15}(PO_4)_2$] were pre-designed, while the L presented larger ion (Sr^{2+} and Ba^{2+}) and S varied among Mg^{2+}, Cu^{2+}, and Co^{2+}. The visual representation of ionic radii of the candidates is shown in Figure S1. In brief, a certain amount of $(NH_4)_2HPO_4$ was dissolved in double distilled water to obtain a 0.5 M solution and ammonia was added to modify the pH to 9.5. Then, same volume solution containing metallic salts under the total concentration of 0.75 M was prepared and rapidly poured into the former solution while maintaining magnetic stirring. Instant milky suspension was observed and extra mixing of 20 min was recommended for homogenization. After vacuum filter and through rinse with water and alcohol (the volume ratio = 2:3), the powder was dried at 28 ± 2 °C for 8 h. In order to identify the effect binary-cation doping played in the thermally induced crystallization and phase evolution of the ACPs, portions of the ACP powder were annealed under different temperatures. The nomenclature of samples was based on the doping cation and annealing temperature. For example, 5Sr5Mg-600 stands for the sample annealed at 600 °C from ACP doped with Sr and Mg. ACP without any designated foreign cations was also prepared and named as sample ACP.

2.3. Material Characterization. The X-ray diffraction (XRD) patterns were collected on a MiniFlex 600 (Rigaku, Japan) with Cu K_α radiation in the scanning range of 10−50° at a speed of 10°/min. Thermogravimetric and differential thermal analysis (TG−DTA) was performed with an STA 449 F3 apparatus (NETZSCH, Germany). The heating rate was 10 °C/min in the range of 30−800 °C. Elemental composition was obtained by inductively coupled plasma−mass spectrometry (ICP−MS) NexION 350X (PerkinElmer, USA).

3. RESULTS AND DISCUSSION

As an initial step, the elemental analysis of prepared ACPs was carried out and summarized in Table 1. The substitution level of foreign cations was in good agreement with the theoretical values except the Cu^{2+}. Such a phenomenon might be related with smaller K_{sp} of $Cu(OH)_2$, which reached as low as 2.2×10^{-20}. The XRD patterns of pristine ACPs are shown in Figure S2a. Evidently, the resulted ACPs remained amorphous regardless of the varieties of foreign cations and no visible sharp peaks were identified.[12]

Table 1. Elemental Ratios of ACPs by Means of ICP−MS[a]

sample name	theoretical M^{2+} amount mol	L/(Ca + L + S)	S/(Ca + L + S)
5Sr5Mg	0.05	Sr 0.047	Mg 0.043
5Sr5Cu	0.05	Sr 0.045	Cu 0.032
5Sr5Co	0.05	Sr 0.047	Co 0.047
5Ba5Mg	0.05	Ba 0.046	Mg 0.043
5Ba5Cu	0.05	Ba 0.043	Cu 0.027
5Ba5Co	0.05	Ba 0.047	Co 0.046

[a]Each sample was triply tested and the margin of error was ≤10%.

In order to understand the role that binary-cation doping played in the thermally induced crystallization of ACP, temperature-dependent XRD analysis and thermal behavior of ACPs were performed simultaneously. The XRD patterns of sample ACP annealed at different temperatures are shown in Figure S2b. The amorphous structure could remain until 600 °C and the obvious coexistence of α/β polymorphs was observed at a higher temperature (650 °C). Dominated beta-TCP with negligible α-TCP composed the XRD pattern of sample ACP-700 and full transformation to β-TCP was completed at around 750 °C. Such tendency agreed with previous research studies, while the composition under specific temperature might be contradictory.[14] Especially, the initial crystalline phase was α/β polymorphs rather than pure α polymorph. Such inconsistence came from the inherent amorphous nature of ACP and was related to the way ACP was synthesized.[8] However, such difference was not the main subject, and the temperature-dependent XRD patterns of sample ACPs were provided for comparison.

Evidently, the binary-cation substitution altered the crystal pathway on the element-dependent behavior (Figure 1). Previous research studies identified that larger cations promoted the formation of α-TCP, while the smaller ones preferred the β-TCP.[14] However, the smaller cations dominated the effect on the crystalline phase when they coexisted, resulting in the formation of pure β-TCP under lower temperature (650 °C) and complete prevention of α-TCP. Noticeable shifts of the positions of reflection peaks would be interpreted as the direct evidence of the incorporation of foreign cations into the crystal lattice of β-TCP.[19] Normally, larger cations tended to inhibit the crystallization of ACP, while the smaller ones promoted. Samples containing Sr showed different degrees of crystallization under 600 °C, while ones containing Ba remained amorphous, which implied that Ba ions possessed the greater potential of maintaining amorphous and might be related to its superior ionic radius. Especially, sample 5Sr5Mg-600 was identified as β-TCP with its sharp diffraction peaks but Ba ion neutralized the effect of Mg ion and maintained amorphous with the case of sample 5Ba5Mg-600. The presence of the Cu ion altered the initial crystalline phase of sample 5Sr5Cu, resulting in weak crystallization of beta-TCP under 600 °C.[18] However, the Cu ion collectively enhances the ability of the Ba ion to remain ACP amorphous, so that the sample 5Ba5Cu could remain amorphous until 650 °C, even more than the Ba ion itself.

TG−DTA curves (Figure 2) were provided to understand the thermally induced crystallization of ACP. The TG−DTG

https://doi.org/10.1021/acsomega.2c07117
ACS Omega 2023, 8, 7602−7606

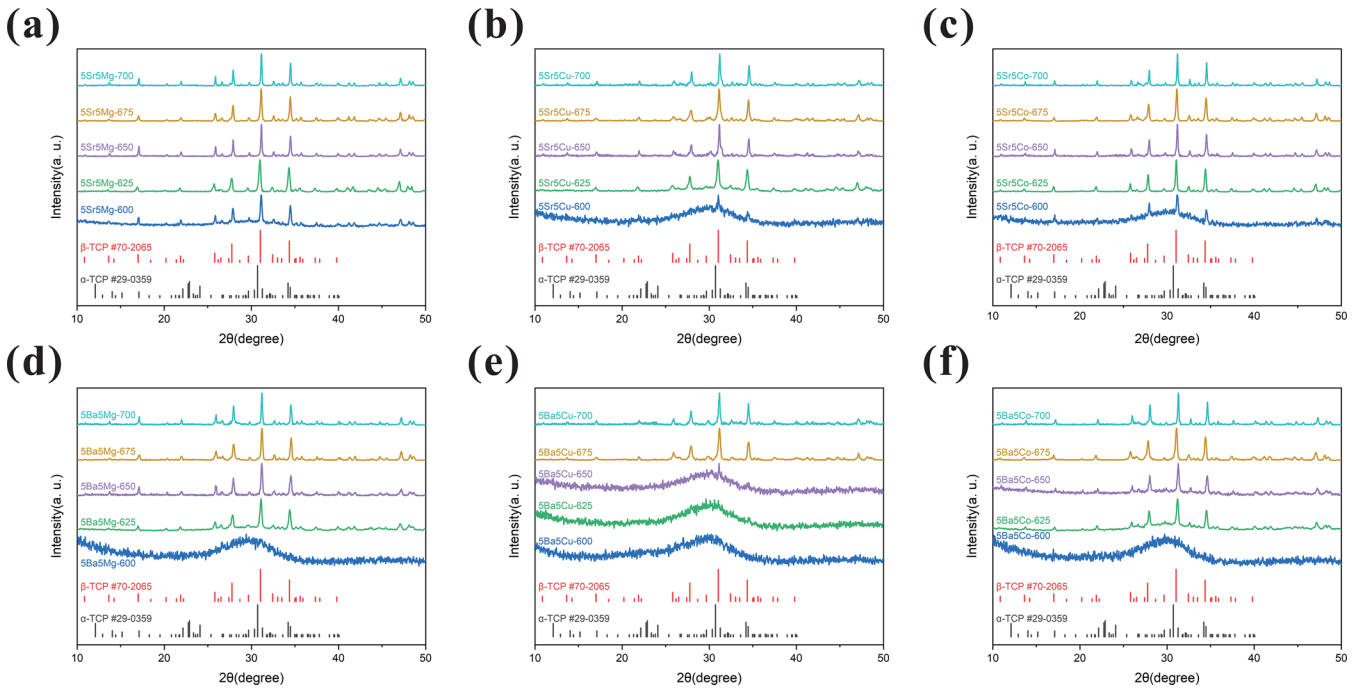

Figure 1. Temperature-dependent XRD patterns of ACPs with binary-cation doping. (a) 5Sr5Mg; (b) 5Sr5Cu; (c) 5Sr5Co; (d) 5Ba5Mg; (e) 5Ba5Cu; and (f) 5Ba5Co.

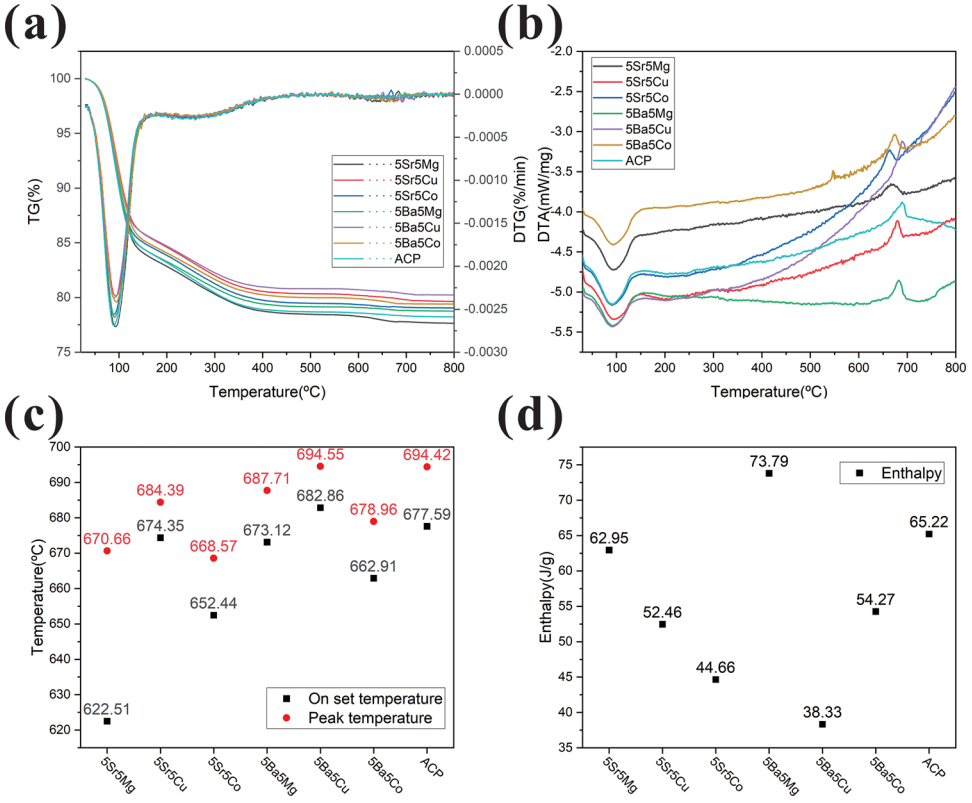

Figure 2. Binary-cation doping modified the thermal behavior of ACP. (a) TG−DTG curves and (b) DTA curves of samples; (c) on set and peak temperatures; and (d) enthalpy of crystallization peaks determined from DTA curves.

results showed the same tendency regardless of the foreign ions. Sample experienced a rapid weight loss at around 100 °C corresponding to the reversible removal of adsorbed water and a slow weight loss at 200−400 °C, suggesting the irreversible removal of chemically bound water. Such a phenomenon was the significant feature of ACP obtained by air drying.[1] The exothermic crystallization effect of ACP toward a higher crystalline phase was analyzed by DTA curve and the characteristic temperature (on-set temperature and peak temperature) and phase transition enthalpy are shown in

https://doi.org/10.1021/acsomega.2c07117
ACS Omega 2023, 8, 7602−7606

Figure 2c,d. The on-set temperature and peak temperature of samples containing Ba were higher than ones of the samples containing Sr, indicating the greater potential of Ba to retard ACP crystallization, which has been proved by the temperature-dependent XRD analysis. Previous study showed that Ba ion could promote the formation of α-TCP and even completely prevent its transition to beta phase up to 1500 °C.[14,20] The lower initial temperature (622.51 °C) and peak temperature (670.66 °C) of sample 5Sr5Mg further verified the thermodynamic factors of better crystallinity at 600 °C. The high initial temperature (682.56 °C) and peak temperature (694.55 °C) of sample 5Ba5Cu implied that it remained amorphous until 650 °C.

4. CONCLUSIONS

This work investigated the thermally induced crystallization of ACP with cosubstitution of larger and smaller divalent cations. Predesigned combination of larger (Sr^{2+} and Ba^{2+}) and smaller (Mg^{2+}, Cu^{2+}, and Co^{2+}) divalent cations were carried out and their effects were outlined. Compared with the single cation doping, the coexistence of larger and smaller divalent ions showed the competition and neutralization of two mechanism. On the one hand, the smaller divalent ions dominated the crystalline phase and shifted the thermodynamic equilibrium toward the β-TCP while completely preventing the formation of α-TCP. On the other hand, the larger divalent ions retarded the crystallization of ACP and maintained the amorphous structure partially or completely until a higher temperature.

■ ASSOCIATED CONTENT

Supporting Information

The Supporting Information is available free of charge at https://pubs.acs.org/doi/10.1021/acsomega.2c07117.

Ionic radii of the selected divalent cations in a six-fold coordination (Figure S1) and XRD patterns of the as-prepared ACPs and temperature-dependent XRD patterns of sample ACP annealed under different temperatures (Figure S2) (PDF)

■ AUTHOR INFORMATION

Corresponding Author

Jianqiang Bi − *Key Laboratory for Liquid-Solid Structural Evolution and Processing of Materials, Ministry of Education, Shandong University, Jinan 250061, People's Republic of China; School of Materials Science & Engineering, Shandong University, Jinan 250061, People's Republic of China*; Phone: +86-531-88396179; Email: bjq1969@163.com

Authors

Lu Wang − *Key Laboratory for Liquid-Solid Structural Evolution and Processing of Materials, Ministry of Education, Shandong University, Jinan 250061, People's Republic of China; School of Materials Science & Engineering, Shandong University, Jinan 250061, People's Republic of China*; orcid.org/0000-0002-9552-7539

Junxing Yang − *Key Laboratory for Liquid-Solid Structural Evolution and Processing of Materials, Ministry of Education, Shandong University, Jinan 250061, People's Republic of China; School of Materials Science & Engineering, Shandong University, Jinan 250061, People's Republic of China*

Kangning Sun − *Key Laboratory for Liquid-Solid Structural Evolution and Processing of Materials, Ministry of Education, Shandong University, Jinan 250061, People's Republic of China; School of Materials Science & Engineering, Shandong University, Jinan 250061, People's Republic of China*

Aimin Li − *Key Laboratory for Liquid-Solid Structural Evolution and Processing of Materials, Ministry of Education, Shandong University, Jinan 250061, People's Republic of China; School of Materials Science & Engineering, Shandong University, Jinan 250061, People's Republic of China*

Junjie Mao − *Key Laboratory for Liquid-Solid Structural Evolution and Processing of Materials, Ministry of Education, Shandong University, Jinan 250061, People's Republic of China; School of Materials Science & Engineering, Shandong University, Jinan 250061, People's Republic of China*

Complete contact information is available at: https://pubs.acs.org/10.1021/acsomega.2c07117

Notes

The authors declare no competing financial interest.

■ ACKNOWLEDGMENTS

The authors would like to thank the staff and postgraduate students at Shandong University for their assistances in carrying out the elementary composition, phase transformation, and thermal behavior. In particular, the authors would like to thank Dr Yongxin Qi and Chen Liu for their heavy testing work. The authors would like to thank Shiyanjia Lab (www.shiyanjia.com) for the assistance at the elementary composition.

■ REFERENCES

(1) Vecstaudza, J.; Gasik, M.; Locs, J. Amorphous calcium phosphate materials: Formation, structure and thermal behaviour. *J. Eur. Ceram. Soc.* **2019**, *39*, 1642−1649.

(2) Dalmônico, G. M. L.; Ihiawakrim, D.; Ortiz, N.; Barreto Junior, A. G.; Curitiba Marcellos, C. F. C.; Farina, M.; Ersen, O.; Rossi, A. L. Live Visualization of the Nucleation and Growth of Needle-Like Hydroxyapatite Crystals in Solution by In Situ TEM. *Cryst. Growth Des.* **2022**, *22*, 4828−4837.

(3) Bertolotti, F.; Carmona, F. J.; Dal Sasso, G.; Ramírez-Rodríguez, G. B.; Delgado-López, J.; Pedersen, J. S.; Ferri, F.; Masciocchi, N.; Guagliardi, A. On the amorphous layer in bone mineral and biomimetic apatite: A combined small- and wide-angle X-ray scattering analysis. *Acta Biomater.* **2021**, *120*, 167−180.

(4) Wang, Z.; Li, Q.; Ren, S.; Zhang, H.; Chen, J.; Li, A.; Chen, Y. Composite monetite/amorphous calcium phosphate bone cement promotes bone regeneration. *Ceram. Int.* **2023**, *49* (5), 7888−7904.

(5) Dorozhkin, S. V. Synthetic amorphous calcium phosphates (ACPs): preparation, structure, properties, and biomedical applications. *Biomater. Sci.* **2021**, *9*, 7748−7798.

(6) Santen, R. A. V. The Ostwald step rule. *J. Phys. Chem.* **1984**, *88*, 5768−5769.

(7) Liu, S.; Weng, W.; Li, Z.; Pan, L.; Cheng, K.; Song, C.; Du, P.; Shen, G.; Han, G. Effect of PEG amount in amorphous calcium phosphate on its crystallized products. *J. Mater. Sci.: Mater. Med.* **2009**, *20*, 359−363.

(8) Wang, L.; Bi, J.; Sun, K.; Li, A.; Yuan, Z.; Yang, F.; Mao, J. Effect of inositol on the thermally induced crystallization and phase evolution of amorphous calcium phosphate. *Crystengcomm* **2022**, *24*, 7193−7199.

(9) Matsunaga, K.; Kubota, T.; Toyoura, K.; Nakamura, A. First-principles calculations of divalent substitution of Ca^{2+} in tricalcium phosphates. *Acta Biomater.* **2015**, *23*, 329−337.

(10) Berg, C.; Unosson, E.; Riekehr, L.; Xia, W.; Engqvist, H. Electron microscopy evaluation of mineralization on peritubular

dentin with amorphous calcium magnesium phosphate microspheres. *Ceram. Int.* **2020**, *46*, 19469−19475.
(11) Sinusaite, L.; Renner, A. M.; Schütz, M. B.; Antuzevics, A.; Rogulis, U.; Grigoraviciute-Puroniene, I.; Mathur, S.; Zarkov, A. Effect of Mn doping on the low-temperature synthesis of tricalcium phosphate (TCP) polymorphs. *J. Eur. Ceram. Soc.* **2019**, *39*, 3257−3263.
(12) Gelli, R.; Briccolani-Bandini, L.; Pagliai, M.; Cardini, G.; Ridi, F.; Baglioni, P. Exploring the effect of Mg^{2+} substitution on amorphous calcium phosphate nanoparticles. *J. Colloid Interface Sci.* **2022**, *606*, 444−453.
(13) Griesiute, D.; Sinusaite, L.; Kizalaite, A.; Antuzevics, A.; Mazeika, K.; Baltrunas, D.; Goto, T.; Sekino, T.; Kareiva, A.; Zarkov, A. The influence of Fe^{3+} doping on thermally induced crystallization and phase evolution of amorphous calcium phosphate. *Crystengcomm* **2021**, *23*, 4627−4637.
(14) Sinusaite, L.; Kareiva, A.; Zarkov, A. Thermally Induced Crystallization and Phase Evolution of Amorphous Calcium Phosphate Substituted with Divalent Cations Having Different Sizes. *Cryst. Growth Des.* **2021**, *21*, 1242−1248.
(15) Sinusaite, L.; Popov, A.; Raudonyte-Svirbutaviciene, E.; Yang, J.-C.; Kareiva, A.; Zarkov, A. Effect of Mn doping on hydrolysis of low-temperature synthesized metastable alpha-tricalcium phosphate. *Ceram. Int.* **2021**, *47*, 12078−12083.
(16) Sinusaite, L.; Antuzevics, A.; Popov, A. I.; Rogulis, U.; Misevicius, M.; Katelnikovas, A.; Kareiva, A.; Zarkov, A. Synthesis and luminescent properties of Mn-doped alpha-tricalcium phosphate. *Ceram. Int.* **2021**, *47*, 5335−5340.
(17) Tong, C.; Zhu, Y. G.; Xu, C. Y.; Yang, L.; Li, Y. D. Luminescence properties and color identification of Eu doped $Ca_3(PO_4)_2$ phosphors calcined in air. *Phys. B* **2017**, *521*, 153−157.
(18) Spaeth, K.; Goetz-Neunhoeffer, F.; Hurle, K. Cu^{2+} doped beta-tricalcium phosphate: Solid solution limit and crystallographic characterization by rietveld refinement. *J. Solid State Chem.* **2020**, *285*, 121225.
(19) Deyneko, D. V.; Fadeeva, I. V.; Borovikova, E. Y.; Dzhevakov, P. B.; Slukin, P. V.; Zheng, Y.; Xia, D.; Lazoryak, B. I.; Rau, J. V. Antimicrobial properties of co-doped tricalcium phosphates $Ca_{3-2x}(M' M'')_x(PO_4)_2$ (M = Zn^{2+}, Cu^{2+}, $Mn^{2+}$and Sr^{2+}). *Ceram. Int.* **2022**, *48*, 29770−29781.
(20) Yashima, M.; Kawaike, Y. Crystal structure and site preference of Ba-doped alpha-tricalcium phosphate $(Ca_{1-x}Ba_x)_3(PO_4)_2$ through high-resolution synchrotron powder diffraction (x=0.05 to 0.15). *Chem. Mater.* **2007**, *19*, 3973−3979.

https://doi.org/10.1021/acsomega.2c07117
ACS Omega 2023, 8, 7602−7606